Environ. Sci. Technol. **2000**, *34,* 680−685

Chromatographic Alteration of a Nonionic Surfactant Mixture During Transport in Dense Nonaqueous Phase Liquid Contaminated Sediment

GAOBIN BAO, W. WYNN JOHN, AND WILLIAM P. JOHNSON*

Department of Geology and Geophysics, University of Utah, Salt Lake City, Utah 84112

Chromatographic alteration of a nonionic surfactant mixture during transport through DNAPL-contaminated aquifer sediment may occur due to differential loss of oligomers to sediment and to dense nonaqueous phase liquid (DNAPL). These losses may significantly alter the solubilizing properties of the mixture, which is a concern when the surfactant mixture is applied for the purpose of DNAPL solubilization. This study examined a nonionic surfactant mixture, which was characterized in terms of oligomer distribution within the mixture and the ability of the mixture to solubilize residual DNAPL. Three sediment-packed columns were connected in series to represent up-gradient, residual, and down-gradient zones, respectively, of a DNAPL-contaminated site. In the up-gradient column, greater retardation of high ethoxylate (EO) content oligomers was observed relative to low EO content oligomers, due to preferential sorption of high EO content oligomers by the sediment. In the residual-zone column, much greater retardation of low EO content oligomers relative to high EO content oligomers occurred, due to preferential sorption of low EO content oligomers to residual DNAPL. In the down-gradient column, retardation of only the high EO content oligomers was observed, due to lack of sorption of low EO content oligomers to sediment. Surfactant losses to sediment and DNAPL delayed the solubilization of DNAPL due to reduction of surfactant concentration and overall increased polarity of the surfactant mixture. Increased solution flow rate decreased surfactant sorption but resulted in an overall decrease in the mass of DNAPL solubilized due to kinetic limitations in DNAPL solubilization.

Introduction

Recent attention has been focused on the loss of nonionic surfactant oligomers from aqueous mixtures to model and natural aquifer sediment (*1*−*5*) and to dense nonaqueous phase liquids (DNAPL) (*6*, *7*). During transport through DNAPL-contaminated sediment, loss of surfactant oligomers by sorption to sediment and DNAPL may occur, and these processes may or may not be kinetically limited under environmentally relevant flow rates. Surfactant loss to either the sediment or DNAPL phases may be dominated by preferential sorption of more or less polar oligomers, depending on the properties of the surfactant mixture, sediment, and the DNAPL (*8*, *9*). Solubilizing properties of the surfactant mixture are subsequently altered by decreased bulk surfactant concentration as well as by changes in the critical micelle concentration (CMC) of the solution as the oligomer distribution within the mixture is shifted (*4*, *10*).

The purpose of this study was to investigate the chromatographic alteration of a nonionic surfactant mixture during transport through low f_{oc} aquifer sediment contaminated by residual tetrachloroethene (PCE). PCE is representative of chlorinated solvents commonly found at DNAPL-contaminated sites. The cumulative changes in the oligomer composition and solubilizing properties of the surfactant mixture were examined as the mixture progressed within a series of three columns representing uncontaminated up-gradient sediment, DNAPL residual-contaminated sediment, and down-gradient sediment, respectively. The interstitial velocity was varied to examine the effect of possible kinetic limitations in surfactant sorption to sediment and DNAPL, and solubilization of DNAPL, on the overall efficiency of solubilization.

Experimental Section

Reagents. A mixture (1:2 by weight) of two octylphenol ethoxylate nonionic surfactants, Igepal CA-720 and Igepal CA-887 (Rhodia, Inc.) with average ethoxylate (EO) chain lengths of 12 and 30 EO units, respectively, was examined. The molecular weights, critical micelle concentrations (CMCs), hydrophilic−lipophilic balance (HLBs), and chemical formulas of these surfactants are reported in John et al. (*8*). Tetrachloroethene (PCE) (Aldrich, reagent grade, 99+%) was used to represent DNAPL. The PCE DNAPL was stained by adding Oil-Red-O (Sigma, Inc.) to 0.01% concentration, which has been shown to not affect PCE dissolution (*11*). Artificial groundwater (AGW) was used in all experiments and was prepared according to Scholl et al. (*12*) as follows: 1.5×10^{-5} M KNO_3, 1.4×10^{-4} M $MgSO_4 \cdot 7H_2O$, 7.0×10^{-5} M $CaSO_4 \cdot 2H_2O$, 8.0×10^{-5} M NaCl, 1.4×10^{-5} M $NaHCO_3$, pH ∼6.8, and ionic strength equal to 3.0 mM.

Column Experiments. Natural aquifer sediment quarried from Pleistocene lacustrine deposits was obtained from Monroc Incorporated (Salt Lake City, UT). The sand was washed with Milli-Q water (Millipore Corp., Bedford, MA) and sieved to remove grains larger than 2 mm and smaller than 106 μm (*8*). The surface area of the sediment (3.273 $m^2 g^{-1}$) was measured by N_2 BET multipoint analysis (Porous Materials, Inc., Ithaca, NY). A total organic carbon analysis (American West Analytical Laboratories, Salt Lake City, UT) measured the sediment organic carbon (f_{oc}) to be 0.0033. Mineralogical and size distribution information for this sand is given in John et al. (*8*).

Three glass chromatography columns (Omnifit, 2.5 cm inside diameter, and 15 cm length) were used. The columns were packed with air-dried sediment. During packing, 10 g additions were vibrated and then pressed by tamping with a rubber stopper 50 times. To avoid entrapment of air during saturation, the columns were flushed with carbon dioxide (highly soluble relative to air) prior to introducing Milli-Q water at a flow rate of 0.5 mL min^{-1}. AGW was subsequently introduced for four pore volumes to equilibrate the columns. After equilibration, PCE DNAPL was introduced to one of the columns in up-flow mode (0.1 mL min^{-1}) for 1.4 pore volumes. AGW was subsequently introduced in down-flow mode for four pore volumes, after which flow direction was reversed for an additional four pore volumes to emplace

* Corresponding author phone: (801)581-5033; fax: (801)581-7065; e-mail: wjohnson@mines.utah.edu.

10.1021/es9908873 CCC: $19.00
Published on Web 01/12/2000

PCE residual. At this point, no nonaqueous phase PCE was observed in the effluent solution of the column.

The pore volume in the columns without PCE residual was determined to be about 21.6 mL by mass difference before and after saturation. The pore volume in the column with PCE residual was determined to be about 16.8 mL, by mass difference before and after residual emplacement, accounting for the density of PCE (1.623 g cm^{-3}). The residual DNAPL content of the column was determined gravimetrically to be ~7.8 g PCE, or ~22% of the pore volume. Tracer (NaBr, 0.001 M) tests were also performed to determine column pore volumes and to determine whether PCE residual blocked advection in water-filled pores, which would cause the advective pore volume to be less than the gravimetric pore volume. The tracer breakthroughs gave column pore volumes that matched those from the gravity estimates for all three columns, indicating that advection occurred throughout the entire water-filled pore space.

Three columns were connected in series to represent up-gradient, residual, and down-gradient zones of a DNAPL-contaminated site. Surfactant solution (2 g L^{-1}, about a factor of 3 above the CMC) was introduced in down-flow mode to initiate the experiment and was continuously introduced to the up-gradient (uppermost) column throughout the experiment. A single clock was used to record time for all three columns during the experiment. Ten percent of the solution flow was split prior to the residual-zone and down-gradient columns to allow collection of samples for GC and HPLC analysis. The experiments were repeated under high (0.3 mL min^{-1}) and low flow rate (0.1 mL min^{-1}) conditions. GC samples were collected from column effluent tubing using a 5 μL-glass syringe for direct injection. After each injection, the syringe was rinsed with water and methanol. HPLC samples were collected using 2 mL autosampler vials (12 × 32 mm, with red PTFE/white silicone and polypropylene closure) and 0.15 mL inserts (for samples from the up-gradient and residual-zone columns). Twenty percent methanol was added into the HPLC samples to prevent the sorption of surfactant to the glass walls of the vials.

HPLC Analyses. Surfactant concentrations were analyzed using a Shimadzu 10Avp high performance liquid chromatography (HPLC) system with a 70-vial autosampler, fluorescence detection, and CLASS-VP 5.021 software. The analytical method utilized was modified from a method developed for nonylphenol ethoxylates (*13*). This reverse-phase method involves the use of a silica column and a C18 precolumn, which allows for underivatized aqueous injections. A detailed description of the HPLC analyses is given in John et al. (*8*). Due to the length of HPLC analysis, HPLC analyses were not replicated.

GC Analyses. PCE concentrations were determined by gas chromatography (Shimadzu GC-17A, with FID detection). The method used was modified from Fountain et al. (*14*) and described in detail in John et al. (*8*).

Data Treatment. Pore volume was not a useful measure of time, since pore volumes differed between the residual-zone column and the other columns, and the goal was to compare surfactant and PCE breakthrough between the three columns. To allow comparison between the columns, measured sampling times were modified by adding to the experimental sampling time the residence times (pore volume divided by flow rate) of tracer in all subsequent columns, to result in what was called equalized time. The effluent concentrations for the three columns at a given equalized time represent concentrations within the same parcel of water exiting each of the three columns. The equalized time was also normalized by the total residence time of water in the entire three-column system (225 and 650 min at the high and low flow rates, respectively) to give time in terms of system pore volumes.

TABLE 1. Surfactant Mass Sorbed and PCE Mass Retarded at the High and Low Flow Rates

		mass sorbed ($\times 10^{-6}$ mol)			
column	velocity (cm/min)	surf (EO > 20)	surf (EO ≤ 20)	total surf	PCE retarded ($\times 10^{-5}$ mol)
up-gradient	0.0572	6.6	5.4	12.0	
	0.1720	3.7	2.5	6.2	
residual-zone	0.0662	0.8	47.9	48.7	3.7
	0.1990	1.7	37.7	39.4	5.4
down-gradient	0.0458	4.7	0.9	5.6	1.0
	0.1376	3.3	0.8	4.1	0.7

Mass of surfactant sorbed in each column was determined by integration of the area above the breakthrough curve to $C/C_0 = 1$ over the period between tracer breakthrough and full surfactant breakthrough, C_0 being the concentration of the bulk surfactant or oligomers in the 2 g L^{-1} stock solution. In cases where full surfactant breakthrough was not achieved, the time of full breakthrough was extrapolated. This extrapolation affected the conclusions negligibly, since in all cases breakthrough to $C/C_0 = 0.9$ or greater was achieved.

The area above the total PCE (dissolved and solubilized) breakthrough curve to $C/C_w^{Sat}{}_{PCE} = 2.06$ (the equilibrium value with 2 g L^{-1} surfactant solution obtained in batch experiments) (*8*) was integrated across the period between tracer breakthrough and complete solubilized PCE breakthrough, to quantify the effects of surfactant sorption and kinetic limitations on dissolution-solubilization on PCE solubilization.

Results and Discussion

Bulk Surfactant Breakthrough. Surfactant breakthrough in the three columns under two interstitial velocities is shown (Figures 1a and 2a) relative to a vertical line representing the mean breakthrough time of a tracer in each of the three columns. Coincidence of the surfactant breakthrough curves with the vertical line would represent conservative surfactant transport through all three columns. Coincidence of surfactant breakthrough curves from two columns would represent conservative surfactant transport in the downstream column. Breakthrough of the surfactant mixture was somewhat retarded relative to a conservative tracer in the up-gradient column (6.2E-6 and 1.2E-5 mol sorbed at high and low flow rates, respectively, Table 1). Greater retardation of surfactant was observed in the residual-zone column (3.9E-5 and 4.9E-5 mol sorbed at high and low flow rates, respectively). Additional retardation of initial surfactant breakthrough was observed in down-gradient column (4.1E-6 and 5.6E-6 mol sorbed at high and low flow rates, respectively). The observed tailing of full surfactant breakthrough in the down-gradient column largely represented sorption that had occurred in the residual-zone column.

The total moles of surfactant sorbed to sediment in the up-gradient column at the low flow rate gives 1.2E-7 mol g^{-1}, which compares favorably to the batch result of 1.3 E-7 mol g^{-1} in equilibrium with a 2.0 g L^{-1} solution of the surfactant mixture (*8*). This result indicates that surfactant sorption to sediment proceeded at equilibrium at the low flow rate. Surfactant sorption to sediment in the up-gradient column was kinetically limited at the higher flow rate, with a 50% decrease in sorbed concentration with a factor of 3 increase in flow rate (Table 1).

The concentration of surfactant sorbed in the residual-zone column was 6.1E-6 mol g^{-1}, which was a much larger value than that observed for batch surfactant sorption to sediment or DNAPL (~2.8E-6 mol g^{-1} sorbed to DNAPL in equilibrium with 2.0 g L^{-1} surfactant solution) (*8*). This is attributable to loss of low EO content oligomers to DNAPL

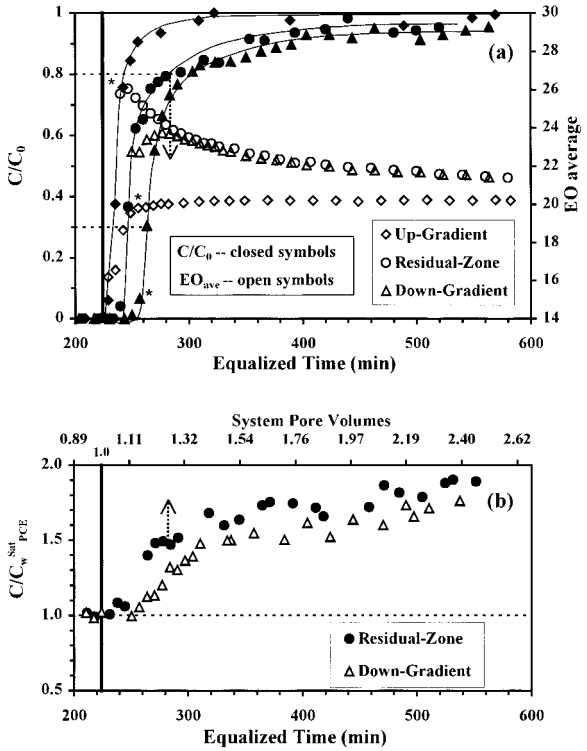

FIGURE 1. Breakthrough of surfactant (a) and PCE (b) in the three columns at high flow rate (0.172 cm min^{-1}). Equalized time (described in text) was used to allow monitoring of cumulative changes in surfactant and PCE concentration as the solution progressed through the three columns. A given location on the *x*-axis represents the same parcel of water exiting the three columns. The vertical line represents the mean breakthrough time of a tracer in each of the three columns. $C_w^{Sat}{}_{PCE}$ represents the solubility of PCE in water. Asterisks show timing of effluent samples analyzed for Figure 3.

(as shown below), since the low EO content oligomers were continuously replenished during the column experiment, whereas their mass was limited in the batch solution. Sorption in the residual-zone column was decreased by 25% when the velocity was increased by a factor of 3, indicating kinetic limitations in surfactant sorption in the residual-zone column at the higher flow rate. Based on the percent change in sorbed mass with changes in flow rate, the kinetic limitations in sorption appeared to be greater in the up-gradient column relative to the residual-zone column, presumably due to differences in the mechanisms of sorption to sediment and DNAPL residual.

Sorption in the down-gradient column was less than that observed in the up-gradient column. The sorbed surfactant concentration achieved in the down-gradient column at the low flow rate was 5.6E-8 mol g^{-1}, which was about 50% lower than the value obtained in the batch experiment (1.3E-7 mol g^{-1}) (*8*), and which was largely attributable to lack of low EO content oligomer (EO < 20) sorption in the down-gradient column (Table 1). The difference between the batch and down-gradient column results at the low flow rate likely cannot be attributed to kinetic limitations on surfactant sorption, since no kinetic limitations at the low flow rate were observed for the other two columns. The relative lack of low EO content oligomer sorption in the down-gradient column may be related to equilibration of that column with high EO content oligomers prior to the introduction of low EO content oligomers as described below. The same effect was not observed in the batch experiment, presumably due to the fact that high and low EO content oligomers were introduced simultaneously as bulk surfactant in the batch experiment. The surfactant mass sorbed in the down-gradient

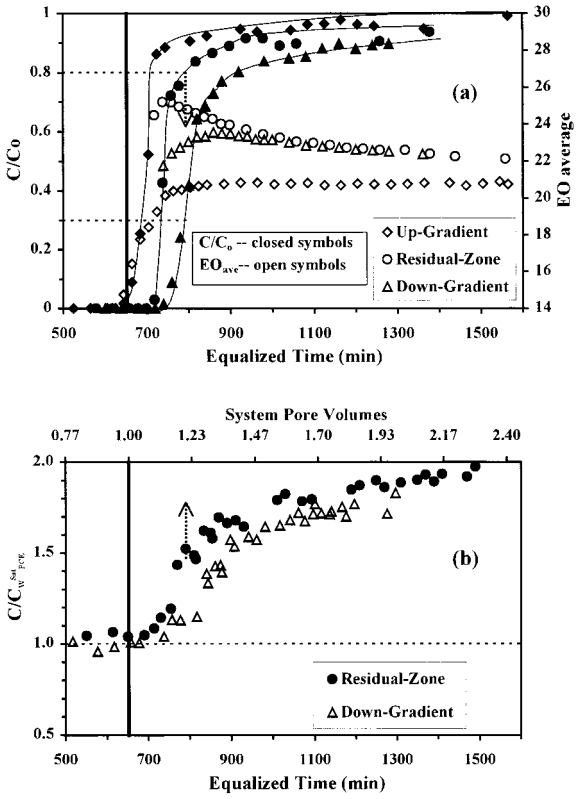

FIGURE 2. Breakthrough of surfactant (a) and PCE (b) in the three columns at low flow rate (0.0572 cm min^{-1}). Figure layout is the same as described in Figure 1.

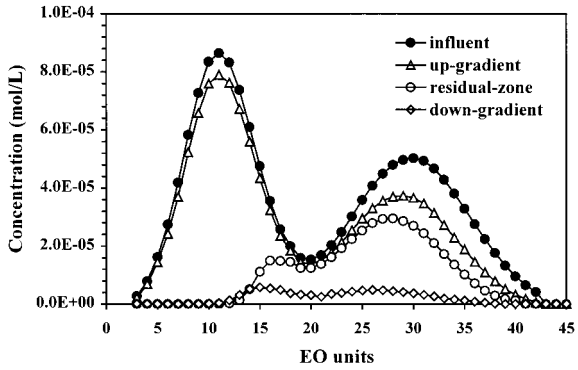

FIGURE 3. Aqueous surfactant concentrations in the influent (to the up-gradient column) and effluent (for all three columns) during initial breakthrough. Asterisks in Figure 1 identify the effluent samples used in this analysis. High EO content oligomers were preferentially sorbed by sediment in the up-gradient column. In the residual-zone column, low EO content oligomers were preferentially sorbed by PCE DNAPL. In the down-gradient column, only intermediate and high EO content oligomers were sorbed.

column decreased about 25% in response to the factor of 3 increase in flow rate (Table 1), a relatively small change compared to the up-gradient column. This may indicate that the dominant mechanism of surfactant sorption to sediment differed between the up-gradient and down-gradient columns.

Oligomer Breakthrough. Up-gradient column EO average curves (Figures 1a and 2a) show that the solution EO average was initially shifted downward relative to the influent solution, due to preferential sorption of high EO content oligomers to the sediment (Figure 3). Figure 3 shows molar concentrations of oligomers in selected samples from each of the column effluents during initial surfactant breakthrough at higher flow rate. Figure 3 indicates that both high and low

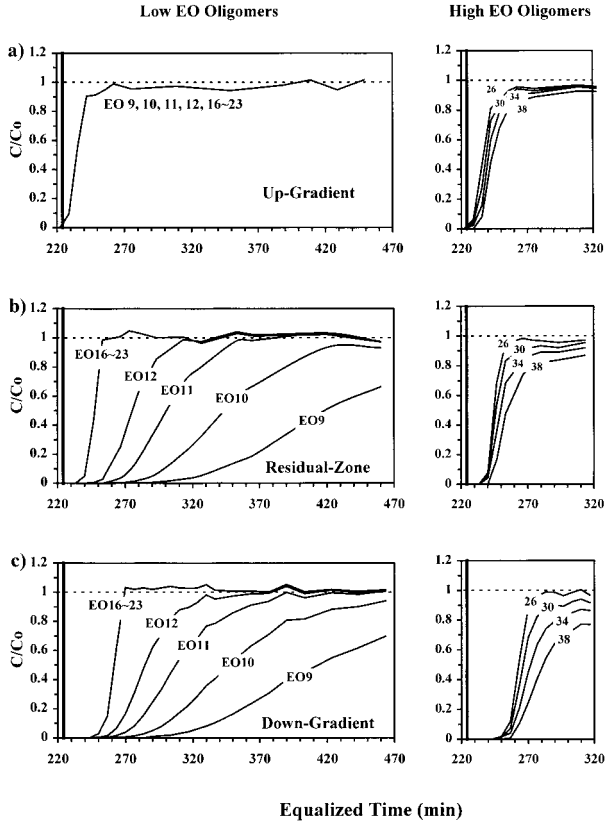

FIGURE 4. Breakthrough of individual surfactant oligomers in the three columns at the high flow rate: (a) up-gradient column, (b) residual-zone column, and (c) down-gradient column. Greater retardation of high EO content oligomers relative to low EO content oligomers was observed in the up-gradient column. In the residual-zone column, low EO content oligomers showed much greater retardation relative to high EO content oligomers. In the down-gradient column, only the intermediate and high EO content oligomers experienced additional retardation. EO16~23 represents all oligomers in the range between EO16 and EO23.

EO content oligomers were sorbed in the up-gradient column, but with greater uptake of high EO content oligomers. As breakthrough progressed (Figure 1a and 2a), the solution EO average in the up-gradient column rose upward and eventually reached the EO average of the influent solution (20.3).

The breakthrough of individual oligomers in the up-gradient column (Figure 4) shows that both low and high EO content oligomers were retarded, with the low EO content oligomers tracing a single breakthrough curve, and the high EO content oligomers showing significant separation during breakthrough (Figure 4a). The greatest retardation of breakthrough was observed for the highest EO content oligomers, indicating the greater affinity of these oligomers for the sediment. The breakthrough data clearly shows the higher relative affinities of the high EO content oligomers for the sediment. In contrast, the sorbed concentrations (determined by integration above the oligomer breakthrough curves) show that the dominant oligomers achieved the highest sorbed concentrations (Figure 5), as was observed in the batch studies (*8*). The sorbed concentrations did not clearly indicate the relative affinities of the oligomers for the sediment, and consideration of only the sorbed concentrations (rather than the breakthrough data) might otherwise have led to an erroneous conclusion that the dominant oligomers would be most strongly retarded during transport through the sediment.

Residual-zone column solution EO averages were initially shifted strongly upward during initial surfactant breakthrough

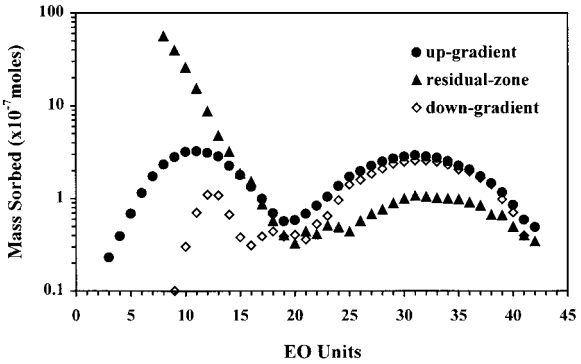

FIGURE 5. EO content oligomer sorption in the three columns after complete surfactant breakthrough in the high flow rate experiment. Oligomer mass sorbed to the sediment was controlled by the oligomer concentrations in the aqueous phase. Low EO content oligomer sorption to PCE DNAPL was controlled by oligomer affinity for that phase, whereas high EO content oligomer sorption to PCE DNAPL was controlled by aqueous oligomer concentration.

(Figures 1a and 2a) due to the preferential uptake of low EO content oligomers by the PCE residual (Figure 3). The solution EO average slowly dropped toward the influent EO average (20.3) (Figures 1a and 2a) as breakthrough of low EO content oligomers in the residual-zone column progressed (Figures 4b and 6).

Low EO content oligomers were strongly retarded in the residual-zone column relative to the up-gradient column, as seen by comparing the breakthrough curves from these two columns (Figures 4 and 6). The lowest EO content oligomers achieved breakthrough last, and the largest separations in the individual breakthrough curves were between the lowest EO content oligomers (Figure 4b), indicating large differences in their relative affinities for the stationary phase, with the highest affinities for the lowest EO content oligomers.

The high EO content oligomers were also retarded in the residual-zone column due to interaction with the stationary phase (Figure 4b). However, since their respective affinities for the stationary phase were similar, the individual high EO content oligomer breakthrough curves showed only slightly increased separation relative to the same curves observed in the up-gradient column (compare 4a and 4b), i.e., they were simply shifted as a group to later times.

Sorption to mineral surfaces (as opposed to PCE residual) in the residual-zone column appeared negligible, although not necessarily nil. This is indicated by Figure 5, where the values and variations in oligomer mass sorbed in the residual-zone column was highest for the lowest EO content oligomers. This result qualitatively matches the batch results for surfactant sorption to PCE DNAPL (*8*), indicating that PCE residual was the dominant sorbent in the residual zone column. The low values and low variation in high EO content oligomer affinities for the DNAPL resulted in the dominant oligomers achieving highest sorbed masses among the high EO content oligomers in the residual-zone column (Figure 5).

Down-gradient column solution EO averages during initial breakthrough (Figures 1a and 2a) were shifted downward relative to that in the residual-zone column, due to preferential sorption of high EO content oligomers to sediment in the down-gradient column (Figure 3). This downward shift was temporary due to the relatively limited additional surfactant retardation in the down-gradient column.

Comparison of oligomer breakthrough curves between the residual-zone and down-gradient columns (Figure 6) shows the effect of oligomer sorption to sediment on the oligomer breakthrough in the down-gradient column. The

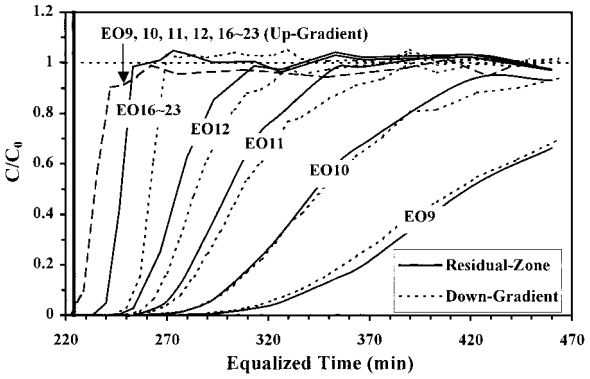

FIGURE 6. Comparison of low EO content oligomers in the three columns at the high flow rate. Low EO content oligomers showed retardation in all three columns. However, the retardation was greatest for the lowest EO content oligomers in the residual-zone column, as seen by comparing breakthrough curves for a given oligomer between the residual-zone and up-gradient columns. In contrast, retardation of lowest EO content oligomers was negligible in the down-gradient, where retardation was greater for the higher content oligomers. This is seen by comparing breakthrough curves for a given oligomer between the down-gradient and residual-zone columns.

lowest EO content oligomers (EO < 11) showed negligible sorption in the down-gradient column, whereas higher EO content oligomers (for example, EO16) showed significant sorption, with sorption increasing with increased EO content of the oligomer as seen by comparing oligomer breakthrough curves from the down-gradient and residual-zone columns (Figure 4 and 6). The high EO content oligomers showed somewhat greater separation during breakthrough in the down-gradient column relative to breakthrough in the residual-zone and up-gradient columns (Figure 4); this presumably resulted from the cumulative effect of preferential sorption of the high EO content oligomers to the sediment.

The sorbed high EO content oligomer concentrations were very similar in the up-gradient and down-gradient columns (Figure 5). In contrast, low EO content oligomer sorption was significant in the up-gradient column (rivaling high EO content oligomer sorption) but was negligible in the down-gradient column (Figure 5). No sorption of oligomers with EO content less than 11 EO units was observed in the down-gradient column, despite low EO content oligomers being present in the aqueous phase after surfactant breakthrough (Figure 6). This indicates that the sediment surface in the down-gradient column was altered relative to that in the up-gradient column. This alteration might somehow be related to the preequilibration of the down-gradient column with dissolved PCE. However, the batch experiments (*8*) indicate otherwise since surfactant sorption was equivalent regardless of whether PCE was present in the aqueous phase. However, the batch results (*8*) do not negate the possibility that sorbed PCE "blocked" sorption of low EO content oligomers, since the batch sediment was not preequilibrated with PCE. Low EO content oligomer sorption has been shown to increase as sediment f_{oc} is increased (*9*). Therefore, it seems unlikely that sorption of PCE would decrease sorption of low EO content oligomers. It is more likely that this alteration is related to the lack of low EO content oligomers in the initial influent to the down-gradient column, which may have allowed high EO content oligomers to fill the available sorption sites. The latter possibility would indicate that low EO content oligomers were not able to compete with high EO content oligomers for sorption sites once the high EO content oligomers were sorbed.

The intermediate EO content oligomers (23 ≥ EO ≥ 16) achieved the fastest transport through the system, being too polar to interact strongly with PCE residual, and too nonpolar to interact strongly with the sediment, as shown in Figure 4c. Although the intermediate EO content oligomers underwent the fastest breakthrough, their ability to solubilize PCE might or might not be greatest relative to the other oligomers, and their relatively low concentration may not even exceed the CMC for the resulting mixture, as described below.

PCE Breakthrough in the Residual-Zone Column. Since surfactant solubilization of DNAPL was the focus of the experiment, the PCE breakthrough curves (Figures 1b and 2b) coincide with surfactant breakthrough, that is, they examine the breakthrough of solubilized rather than dissolved PCE. The concentration of dissolved PCE exiting the residual-zone column was equal to solubility (~190 mg L^{-1}) at both flow rates, indicating no kinetic limitation on PCE dissolution into surfactant-free water at both flow rates.

Solubilized PCE breakthrough was retarded relative to tracer breakthrough (shown by the vertical line) in the residual-zone column due to surfactant interaction with sediment in the up-gradient column and PCE residual in the residual-zone column (Figures 1b and 2b). Initial breakthrough of solubilized PCE was delayed by between 0.1 and 0.2 system pore volumes, and full breakthrough was delayed for more than two system pore volumes (Figures 1b and 2b). The CMC of the influent solution was 0.6 g L^{-1} (*8*) which is represented in Figures 1a and 2a by $C/C_0 = 0.3$. Initial breakthrough of solubilized PCE in the residual-zone column was simultaneous to the breakthrough of surfactant at $C/C_0 = 0.3$, at both high and low flow rates (compare Figures 1a and 2a to Figures 1b and 2b, respectively).

A surfactant concentration of $C/C_0 = 0.8$ represents 70% of full micellization (70% of the difference between the CMC and the influent concentration), which is shown by the downward pointing arrows in Figures 1a and 2a. At this surfactant concentration, the solubilized PCE concentration achieved only about 50% of the full solubilization by 2 g L^{-1} surfactant mixture, as determined by the batch experiments (*8*). This is indicated in Figures 1b and 2b by upward pointing arrows corresponding to those in Figures 1a and 2a. The lag in breakthrough of solubilized PCE behind surfactant breakthrough presumably resulted from the loss of low EO content oligomers to the DNAPL residual, which would have caused the surfactant mixture to be relatively polar during initial breakthrough. Recall that the solution EO average rose about 5 units during initial surfactant breakthrough (Figures 1a and 2a). A relatively polar mixture would be less capable of solubilizing PCE (*6*). This effect was not observed in the batch solubilization experiment (*8*) due to the small rise in solution EO average in that experiment. As breakthrough progressed, the solution EO averages slowly approached that of the influent solution (Figure 1a and 2a), and equilibrium solubilization ($C/C_w^{Sat}{}_{PCE} = 2.06$) was approached (Figures 1b and 2b).

Retardation of solubilized PCE breakthrough was quantified and expressed in terms of retarded mass of PCE (Table 1), as described earlier. In the residual-zone column, the mass retarded at the lower flow rate (3.7E-5 mol) was 68% of the mass of PCE retarded at the higher flow rate (5.4E-5 mol), despite greater surfactant sorption at the lower flow rate. This may indicate kinetic limitations on PCE dissolution-solubilization at the higher flow rate. Kinetic limitations were indicated by a somewhat lower solubilized PCE concentration at the higher flow rate relative to the lower flow rate at two system pore volumes (compare Figures 1b and 2b). Kinetic limitations in PCE solubilization-dissolution by a nonionic surfactant mixture were observed by Pennell et al. (*15*), for a similar interstitial velocity (0.0275 cm min^{-1}).

PCE Breakthrough in the Down-Gradient Column. Solubilized PCE breakthrough in the down-gradient column

showed increased retardation (1.0E-5 mol and 0.7E-5 mol at the low and high flow rates, respectively) relative to the residual-zone column, due to the loss of high EO content oligomers to the sediment. These values were about 26% and 13% (low and high flow rates, respectively) of the values in the residual-zone column. In contrast to the residual-zone column, increased flow rate in the down-gradient column reduced solubilized PCE retardation in that column. This occurred because kinetic limitations affected only surfactant sorption in the down-gradient column. In contrast, kinetic limitations in PCE dissolution in the residual-zone column superimposed upon kinetic limitations in surfactant sorption, resulted in overall increased retardation of solubilized PCE breakthrough as flow rate increased in that column. It should be noted that the distribution of the solute between the micellar solution and the stationary phase might also be an important consideration in the down-gradient column, especially for more hydrophobic solutes, were it not for the preequilibration of dissolved solute with the sediment in this column prior to surfactant breakthrough.

Implications. This work showed that delay of PCE recovery due to surfactant loss to sediment and DNAPL in the up-gradient and residual zones was greater than two system pore volumes and was increased further by surfactant loss to down-gradient sediment, indicating that such delays might be significant in field-scale remediation of nonaqueous contaminant in general. Increased flow rate was shown to decrease surfactant loss to sediment and DNAPL but with greater decreases for sediment (~50%) relative to DNAPL (~20%) for a 3-fold increase in velocity. Increased flow rate resulted in an overall increased delay in contaminant recovery despite less surfactant loss, due to kinetic limitations in DNAPL dissolution-solubilization. Loss of low EO content oligomers to DNAPL in this system increased the polarity of the surfactant mixture and decreased the solubilizing capacity of the mixture. This detrimental effect can be expected to occur in field-scale remediation, to extents depending upon the composition of the nonionic surfactant mixture and the properties of the DNAPL and the sediment. Loss of low EO content oligomers from solution as the mixture progressed through the system, and subsequent equilibration of sediment with high EO content oligomers resulted in decreased sorption of low EO content oligomers to down-gradient sediment. This result indicates preflooding of an aquifer by high EO content oligomers prior to introduction of a nonionic surfactant mixture would reduce or eliminate loss of low EO content oligomers to sediment.

Acknowledgments

The authors very much appreciate the assistance of Dr. Jennifer Field in supplying purified alkylphenol ethoxylate standards for calibration and for helpful conversations during the course of this work. The authors would also like to thank Dr. Tohren C. G. Kibbey for many helpful discussions. Thanks to Dr. Craig Forster for his help in drafting the oligomer breakthrough figures. Funding for this research was provided by the U.S. Environmental Protection Agency under Grant R826650-01 to Dr. W. P. Johnson. This paper has not been subjected to the U.S. Environmental Protection Agency's required peer and policy review and therefore does not necessarily reflect the views of the Agency, and no official endorsement should be inferred.

Literature Cited

(1) Brownawell, B. J.; Chen, H.; Zhang, W.; Westall, J. C. *Environ. Sci. Technol.* **1997**, *31*, 1735−1741.
(2) Yuan, C.; Jafvert, C. T. *J. Contam. Hydrol.* **1997**, *28*, 311−325.
(3) Kibbey, T. C. G.; Hayes, K. F. *J. Colloid Interface Sci.* **1998a**, *197*, 198−209.
(4) Kibbey, T. C. G.; Hayes, K. F. *J. Colloid Interface Sci.* **1998b**, *197*, 210−220.
(5) Johnson, W. P.; John, W. W. *J. Contam. Hydrol.* **1999**, *35*, 343−362.
(6) Zimmerman, J. B.; Kibbey, T. C. G.; Cowell, M. A.; Hayes, K. F. *Environ. Sci. Technol.* **1999**, *33*, 169−176.
(7) Butler, E. C.; Hayes, K. F. *Water Res.* **1998**, *32*, 1345−1354.
(8) John, W. W.; Bao, G.; Johnson, W. P.; Stauffer, T. B. *Environ. Sci. Technol.* **2000**, *34*, 672−679.
(9) Kibbey, T. C. G.; Hayes, K. F. *J. Contam. Hydrol.* **2000**, *41*, 1−22.
(10) Warr, G. G.; Grieser, F.; Healy, T. W. *J. Phys. Chem.* **1983**, *87*, 4520−4524.
(11) Pennell, K. D.; Pope, G. A.; Abriola, L. M. *Environ. Sci. Technol.* **1996**, *30*(4), 1328−1335.
(12) Scholl, M. A.; Mills, A. L.; Herman, J. S.; Hornberger, G. M. *J. Contam. Hydrol.* **1990**, *6*, 331−336.
(13) Kibbey, T. C. G.; Yavaraski, T. P.; Hayes, K. F. *J. Chrom.* **1996**, *752*, 155.
(14) Fountain, J. C.; Starr, R. C.; Middleton, T.; Beikirch, M.; Taylor, C.; Hodge, D. *Ground Water* **1996**, *34*, 910−916.
(15) Pennell, K. D.; Jin, M.; Abriola, L.; Pope, G. A. *J. Contam. Hydrol.* **1994**, *16*, 35−53.

Received for review August 2, 1999. Revised manuscript received November 29, 1999. Accepted December 1, 1999.

ES9908873